Gray, D., Xin, X., Zhu, Y., and le Kernec, J. (2014) Structural slotted waveguide antennas for multirotor UAV radio altimeter. In: 2014 IEEE International Conference on Signal Processing, Communications and Computing (ICSPCC), Guilin, 5-8 Aug. 2014, pp. 819-824. ISBN 9781479952724.

Structural slotted waveguide antennas for multirotor UAV radio altimeter

D. Gray
Dept. Electrical & Electronic Eng.,
Xi'an Jiaotong Liverpool University,
Suzhou, Jiangsu, China
derek.gray@xjtlu.edu.cn

X. Xin, Y. Zhu
NIMTE,
Chinese Academy of Sciences,
Ningbo, Zhejiang, China
y.zhu@nimte.ac.cn

J. Le Kernec
Dept. Electrical & Electronic Eng.,
University of Nottingham,
Ningbo, Zhejiang, China
julien.lekernec@nottingham.edu.cn

***Abstract* — Z-slots are presumed to offer a structural advantage over conventional inclined slots for narrow wall slotted waveguide antennas, in that the corners of the rectangular waveguide are not cut and consequently will not weaken a structural tube as much. Initial structural simulations are shown to confirm this assumption. This slot configuration was also further investigated as radiating slots in standing wave type slotted waveguide antennas. Fan-beam antennas having 10 to 30 slots were successfully designed for 10GHz using a commercially available antenna simulator, having directivities from 16 to 21dBi and aperture efficiency of 60%.**

***Index Terms* — slotted waveguide antennas**

I. INTRODUCTION

Small multi-rotor "helicopter" unmanned aerial vehicles (UAVs) are self-stabilizing flying platforms capable of hovering or low speed flight for periods of up to 40 minutes. These flight characteristics make these small UAVs perfect for high quality photography, such as for real estate. To date, these small UAVs have not been used for radio frequency applications, possibly due to the limited endurance. However, in an educational context where restricted flight time is not an operational impediment, these small UAVs are attractive for student projects on radio frequency sensing and radar; students are engaged by been able to interact with an actual UAV and likewise find the opportunity to work on a system to be integrated with the UAV exciting. Commercially available small mass X-band and 24GHz FMCW radar units make radio frequency systems and machine vision projects possible for undergraduate students.

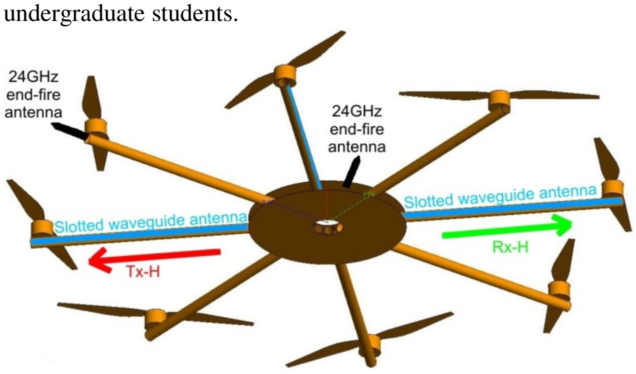

Fig. 1. Multi-rotor unmanned aerial vehicle, with downward looking X-band structurally integrated slotted waveguide antennas and sideward looking 24GHz discrete end-fire antennas for ranging.

It has been noted that long endurance, low altitude maritime patrol is one application where fully autonomous flights of fixed wing UAV could be allowed [1]; there is minimal risk of encountering other low altitude aircraft over blue water, so the UAV would not be remotely piloted nor would there be any human supervision required. In this case, isolation from population centers and extreme geographical isolation both drive and legally enable full automation. Conversely, at the other extreme, full automation appears to be necessary for flying multirotor UAVs in the most densely populated, high rise urban environments for building exterior inspection, post-fire and post-earthquake building interior/exterior inspection, first responders overwatch and environmental monitoring. At present, urban pollution monitoring is restricted to the ground [2].

Crucial to this second application of fully autonomous small UAVs, is the availability of dependable sensors to accurately position the multirotor UAV relative to the ground below and the nearest high rise building walls to the sides. As GPS suffers multipath and is easily jammed, and GPS data for high rise apartment buildings will not always be available, navigation by GPS and onboard solid state inertial sensors for fully autonomous flight amongst high rise buildings is not considered to be feasible. Ultrasonic and passive and active infrared sensors will be adversely affected by smog, smoke, fog, light rain, wind and vortices around high rise buildings. In contrast, radar can provide the required accuracy and dependability in all but the most extreme weather conditions. The availability of low cost, mass-produced X-band and 24GHz FMCW radar units capable of ranging enables the development of bench top prototype and pre-flight radio altimeters by undergraduate project students.

Considering a multirotor UAV on a building inspection or environmental monitoring flight amongst 20 to 30 story apartment buildings, it is likely that for most of the flight that the UAV will be much closer to the nearest building than the ground. With a longer propagation distance to the ground, a longer wavelength radio altimeter would be more appropriate. To this end, the integration of X-band, medium gain, fan beam antennas into the booms/arms of a 1.2m diameter multirotor UAV is being investigated, Figure 1, from both electromagnetic and structural perspectives [4, 5]. To date, it appears that the booms can be used as downward-looking 15 to 16dBi, X-band, fan beam antennas, which will avoid the weight penalty and shortened flight time of carrying equivalent discrete antennas (and appropriate brackets to attach to the chassis) for the same functionality.

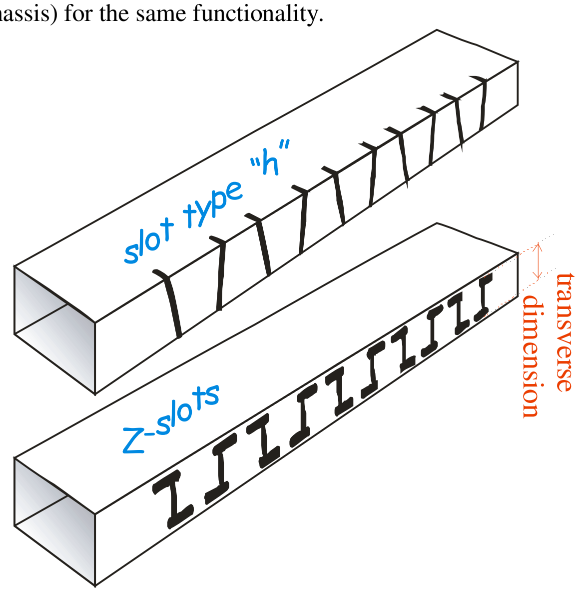

Fig. 2. Sketches of narrow wall 10-slot WR-90 slotted waveguide antennas.

Narrow wall slotted waveguide antennas date from the early 1940s [6, 7], and are used extensively in civil marine radar. For lower X-band, resonant slot lengths exceed the narrow wall height of WR-90 waveguide causing the corners of the rectangular tube to be cut as the slot wraps around, Figure 2. Based on structural studies of broad wall longitudinal slotted waveguide antennas [8], the short ends of the slots on the broad walls of the type "h" narrow wall antennas were considered to be potential severe stress points that will seed broadwall cracking under loading, while having cut the corners of the rectangular tube was considered to significantly structurally weaken the tube; this was the motivation for the development of a novel narrow wall confined Z-slot design [4]. A double slot design such as [9, 10] would be an absolute worst case as a load bearing antenna. It was later found that the narrow wall confined Z-slot was studied for travelling wave type narrow wall slotted waveguide antennas [11, 12], and was declared to be unsuitable for resonant (standing wave) type antennas. It is noted that the C-slot may also be a viable alternate narrow wall confined slot [13].

Having previously demonstrated 10 Z-slot resonant type antennas [4], the next steps were to investigate the mechanical behavior in both aluminum WR-90 waveguide and custom made plain weave carbon fiber reinforced plastic (CFRP) WR-90 sized tubes, and then to increase the number of slots to 30 to rival the travelling wave work reported in [11].

II. Mechanical Analysis of WR-90

The outer diameter of the CFRP cylindrical tubes used as booms to connect the motors/propellers to the central hub of a 1.2 meter diameter multi-rotor UAV is approximately 20mm while the wall thickness is approximately 3mm. These dimensions are close to standard WR-90 rectangular waveguide; internal dimensions 22.86x10.16mm with 1.27mm wall thickness. It is 320mm from the bracket on the central hub to end of the tube, Figure 3. The boom was considered to be a cantilever, been fixed at one end to the central hub while the other end is pulled above the horizontal plane by the motor/propeller. In this initial work, it was assumed that the loading on each boom was 1kg [5].

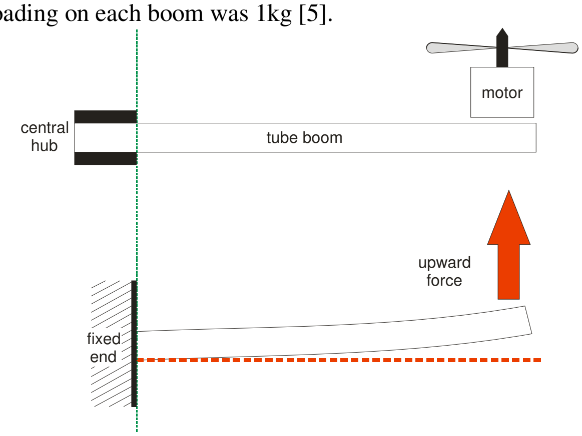

Fig. 3. Multi-rotor UAV arm boom as a cantilever.

When using WR-90 waveguide as a boom, as it is a rectangular tube, it can be mounted with either a broad wall facing downwards or with a narrow wall facing downwards. Either configuration can be used as a downward facing slotted waveguide antenna for X-band radio altimeter. CFRP broad wall slotted waveguides having been reported in [8, 14].

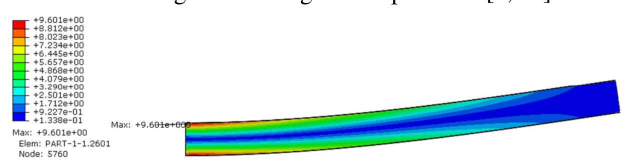

Fig. 4. Simulated von Mises stress field of WR-90 tube, 0.75mm wall thickness CFRP, narrow wall facing downward, without slots, maximum value 9.6MPa; from Abaqus™.

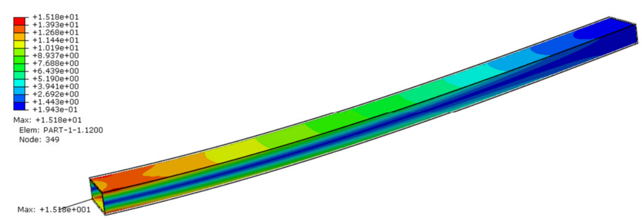

Fig. 5. Simulated von Mises stress field of WR-90 tube, 0.75mm wall thickness CFRP, broad wall facing downward, without slots, maximum value 15.1MPa; from Abaqus™.

As an initial exercise, the 320mm length 0.75mm wall thickness CFRP tube was simulated in the commercially available Finite Element Analysis software Abaqus™. For the narrow wall facing downward configuration, the maximum von Mises stress was 9.6MPa, Figure 4. With a broad wall facing downward, the maximum von Mises stress was 15.1MPa, Figure 5. In terms of von Mises stress, the narrow wall facing downward was best structurally, also presents the lesser dimension to the airflow from the propellers and consequently lower drag. Based on these numerical results, narrow wall slotted waveguide antennas were investigated for downward facing radio altimeter.

A path from the fixed end to the loaded end was defined along the upward facing narrow wall of the WR-90 sized CFRP tube, and the deformation of that path was plotted, Figure 6. The deformation curve resembles a theoretical cantilever, confirming that the boom acts as a cantilever despite been a rectangular tube (hollow beam).

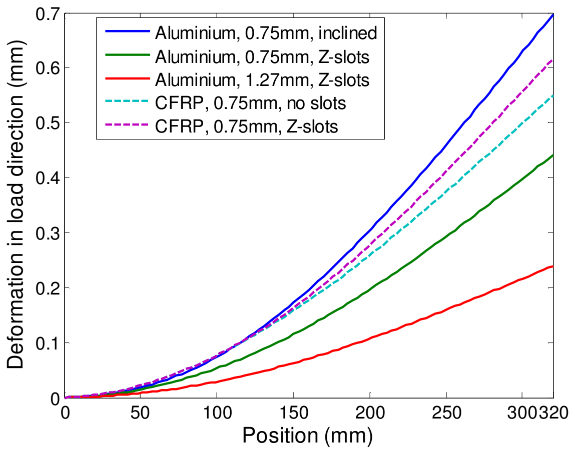

Fig. 6. Simulated deformation along the upper narrow wall WR-90 tubes with 1kg loading at position 320mm, narrow wall facing downward configuration, 0.75mm and 1.27mm wall thickness, CFRP and aluminum, from Abaqus™.

III. Z-slot Slotted Waveguide Antenna Designs

In the initial work on this project, round ended 10 Z-slot antennas were designed and simulated in the commercially available antenna simulation software FEKO™ [4]. As square ended slots have been successfully laser cut, the round ended Z-slots were abandoned. The chief advantage of square ended slots over round ended been a significant reduction in mesh size and simulation time. However, care was still taken to ensure that the inner surface of each slot was meshed so that there were 2 or 3 mesh triangular elements to ensure reasonable accuracy in modelling of the slot currents.

Two considerations motivated the investigation of Z-slot antennas for slot numbers beyond 10. Firstly, the prior work [11, 12] made claims that the Z-slot had insufficiently high impedance to be used in resonant – standing wave type slotted waveguide antennas; designing and demonstrating a 20 or 30 Z-slot antenna would debunk the prior negative claims. Secondly, and more practically, given that the exposed boom length is 320mm for the 1.2meter diameter multi-rotor UAV and that the length of the 10GHz 10-slot antennas is 190mm, there is potentially sufficient boom length to accommodate 18 Z-slot antennas. Designs for 10 to 30 Z-slot antennas are presented in this section.

The general features of narrow wall slotted waveguide antennas are well understood [6, 7]; the slot-to-slot spacing is half a guided wavelength. Consequently, the problem of finding the resonant slot length under the influence of mutual coupling for a particular slot configuration, desired number of slots and given operating frequency is a well constrained problem suitable for automated optimization. The Simplex Nelder-Mead Method optimizer in FEKO™ proved to be near flawless in this work; the optimizer determined appropriate Z-slot length and corner tab length for each different numbers of slots [4].

Two different transverse dimensions were trialed: 9.0mm and 9.6mm, Figure 2. The latter taking up the majority of the width of the inner dimension of the WR-90 inner wall. The maximum number of slots investigated here was 30, in order to rival the larger travelling wave design reported in [11]. This 30 Z-slot antenna had a peak directivity of 21.0dBi, E-plane 3dB beamwidth of 2.5°, H-plane 3dB beamwidth of 98.1°, E-plane sidelobes below -13.2dB below peak and E-plane cross-pol below -20dB below peak, Figure 7. The cross-pol of the Z-slot antennas was significantly lower than that of the equivalent conventional “h” inclined slot antennas, Figure 2. The FEKO™ simulations of this antenna used 32GBytes of RAM and required 35minutes for each frequency step on a 6 CPU machine.

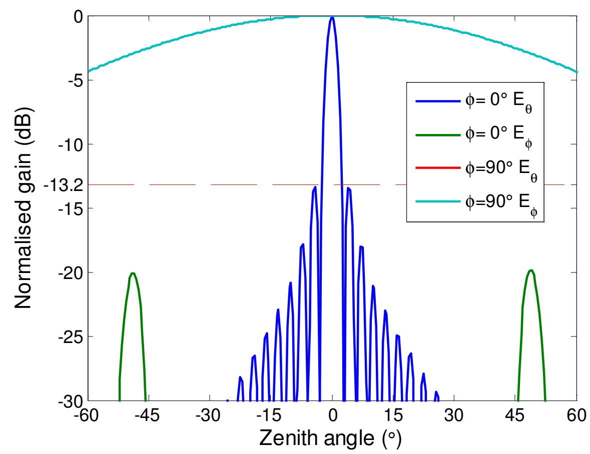

Fig. 7. Radiation pattern of 30 Z-slot narrow wall slotted waveguide antenna at 10GHz; transverse dimension 9.0mm, from FEKO™.

The peak directivity of the 10 to 30 Z-slot designs at 10GHz were found to follow the theoretical 60% aperture efficiency curve closely, Figure 8. As the number of slots was increased, the directivity got closer to the 60% curve, but the effect was very small. It is concluded any transverse electric standing waves on the exterior of the WR-90 waveguide had a consistent effect. The standing wave effects are of concern for mounting the antennas during radiation pattern measurements.

To further confirm the soundness of the optimizer designed antennas before construction and testing, the E and H-plane 3dB beamwidths and E-plane sidelobe levels were extracted. As length of the antennas increased, the E-plane 3dB beamwidth narrowed in a consistent manner, Figure 9. As the antennas are always one slot in length in the H-plane, the H-plane 3dB beamwidth should be a fixed value irrespective of antenna length, and this was found to be the case, Figure 10. As only a uniform aperture illumination was used in the designs, the first E-plane sidelobe level of any antenna should be the rectangular aperture theoretical value of -13.2dB, which was found to be the case, Figure 11. Thus, all the antenna designs were judged to be sound.

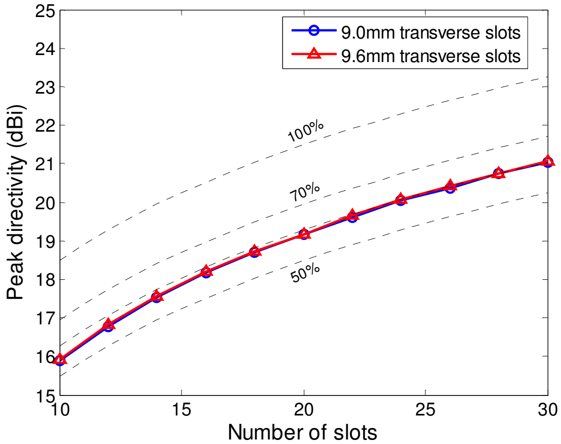

Fig. 8. Variation of 10GHz peak directivity with increasing number of slots, for transverse dimensions of 9.0mm and 9.6mm, theoretical aperture efficiency curves marked as dashed lines; from FEKO™.

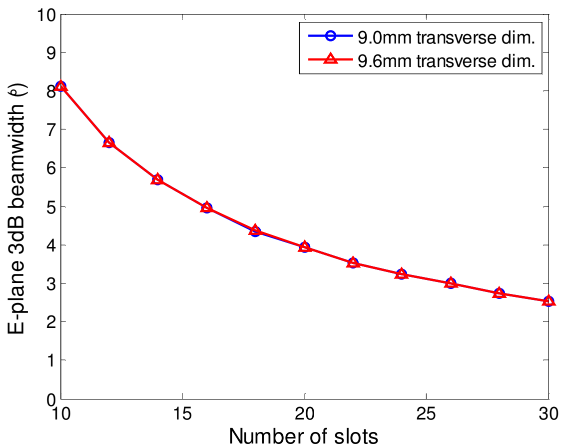

Fig. 9. E-plane 3dB beamwidth variation with increasing number of slots at 10GHz, from FEKO™.

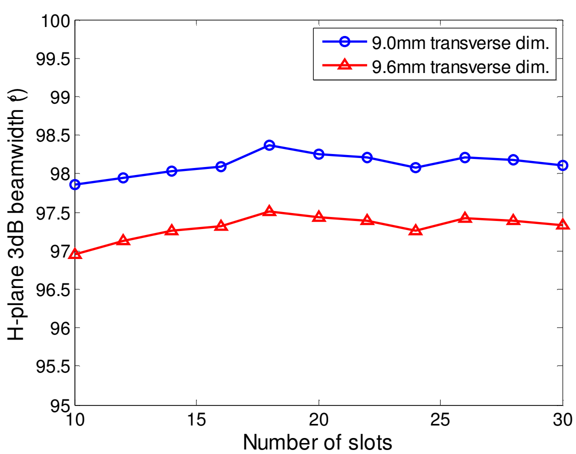

Fig. 10. H-plane 3dB beamwidth variation with increasing number of slots, from FEKO™.

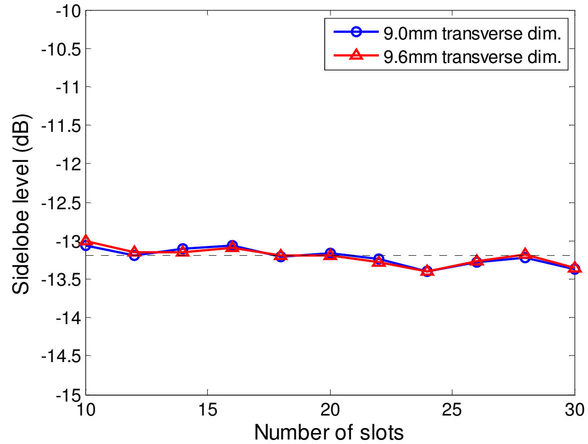

Fig. 11. E-plane sidelobe level variation with increasing number of slots at 10GHz, from FEKO™.

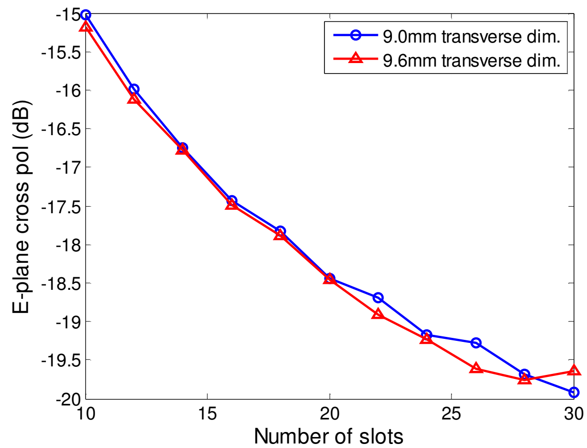

Fig. 12. Decrease of E-plane cross-polarized peak relative to peak directivity with increasing number of slots; from FEKO™.

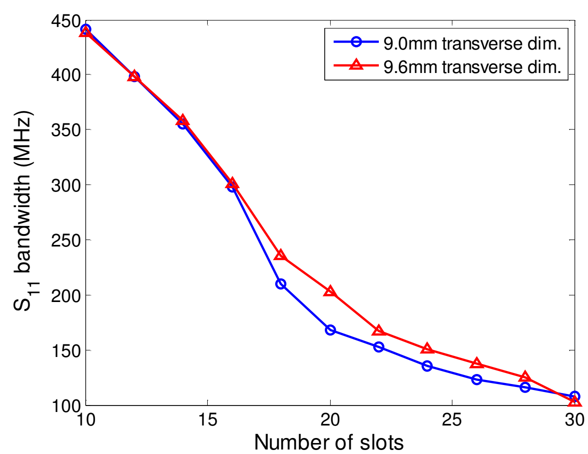

Fig. 13. Variation of $S_{11} \leq$ -10dB bandwidth with increasing number of slots; from FEKO™.

As with conventional narrow wall type "h" slotted waveguide antennas [4], the peak cross-pol radiation occurred in the E-plane of the Z-slot antennas. This was found to decrease with increasing antenna length, Figure 12.

The full series of 10 to 30 Z-slot designs for transverse dimensions of 9.0 and 9.6mm were simulated across 9.5 to 10.5GHz, and figures of merit extracted. As the number of slots was increased, both the return loss $S_{11} \leq -10$dB and the directivity bandwidths narrowed, Figures 13 to 15.

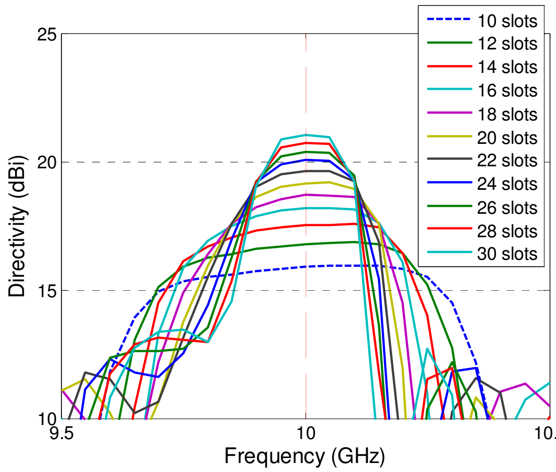

Fig. 14. Frequency dependence of peak directivity, for 9.0mm transverse dimension slots; from FEKO™.

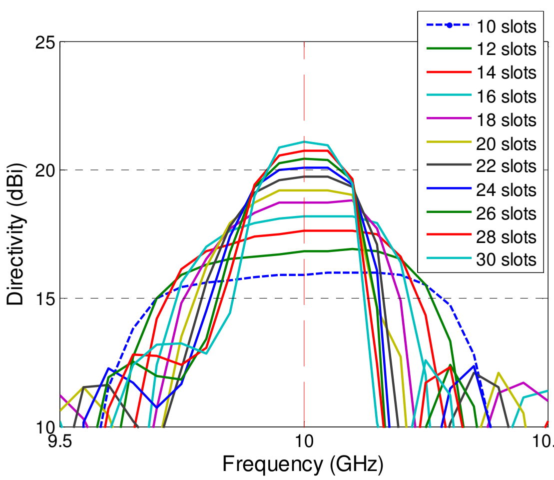

Fig. 15. Frequency dependence of peak directivity, for 9.6mm transverse dimension slots; from FEKO™.

IV. Ranging Accuracy Assessment

Although the narrow wall Z-slot antennas are promising candidates for phased array elements, the immediate interest is as structural boom X-band antennas for radio altimeter for multirotor UAVs. For this application, some estimate of the ranging accuracy was needed before undertaking preflight ground based testing of the radio altimeter. For this initial assessment, the directivity and transmission loss from the FEKO™ models were used to generate 3dB received gain bandwidths from which the range resolution was calculated, Figure 16. The 10 slot antennas gave superior performance with a resolution of 25cm, while the resolution progressively worsens to 115cm for a 30 slot antenna due to the narrowing bandwidth. Due to the better electrical performance, the 10 slot antennas were investigated as load bearing structures.

It is noted that with stretch processing, the resolution of the 10 slot antennas could be improved to 3cm and 9cm for the 30 slot antennas, which will be investigated in the future.

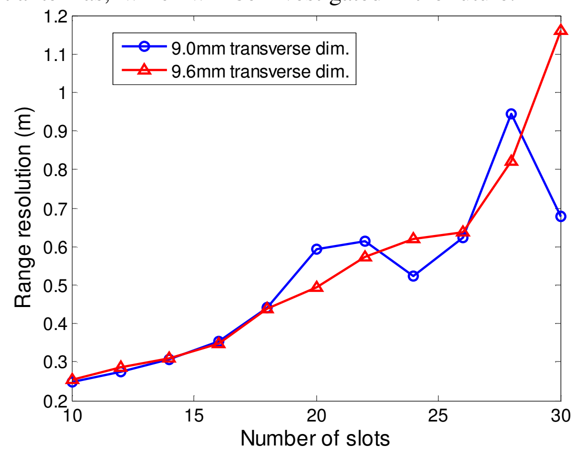

Fig. 16. Range resolution variation with increasing number of slots, calculated from $S_{11} \leq -10$dB bandwidth from Figure 15 and directivity of Figures 16 and 17.

V. Mechanical Analysis of 10 Slot Antennas

Cutting the 10 Z-slots in the narrow wall of the 0.75mm wall thickness CFRP tube close to the load end caused the maximum von Mises stress to increase from 9.6MPa to 27.2MPa, Figures 4 and 17. The stress pattern of the slotted tube still had the same general distribution in that the maximum tension and compression and minimum deformation were at the fixed end, Figure 6. The slotted tube deformed about 0.1mm more than the unslotted tube, with the difference starting at about position 140mm around the 3rd slot, Figure 6. Cutting the slots made the outer half of the CFRP tube more prone to deformation, although this was not a significant change compared to the unslotted tube and could be used as a boom on the multirotor UAV without adding thickness to the tube walls.

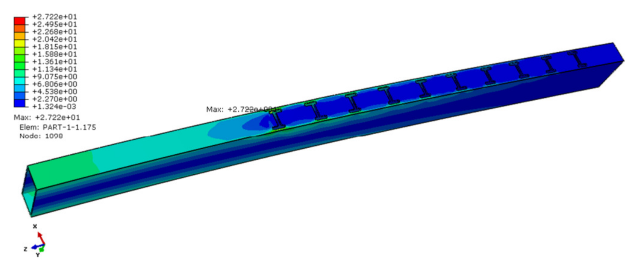

Fig. 17. Simulated von Mises stress field of WR-90 tube with 10 Z-slots close at the loaded end, 0.75mm wall thickness CFRP, narrow wall with slots facing downward, maximum value 27.2MPa; from Abaqus™.

As aluminum has isotropic properties, it was more convenient to compare the type “h” and Z-slot antennas in Abaqus™, Figures 2 and 6. With 0.75mm wall thickness, the type “h” slotted tube deformed 0.7mm while the Z-slotted tube deformed 0.43mm. The structural weakening caused by cutting the Z-slots is less, but under the loading conditions considered, either would be acceptable.

In prior work on broad wall slotted waveguide antennas, 1.5mm diameter grinding bits were used to cut out the slots in CFRP tubes [14, 15]; an endmill bit as would be used on copper or aluminum WR-90 tubing been unsuitable due to the abrasive nature of the CFRP. Here, a laser was used to cut the Z-slots, Figure 18. This required care so as not to burn away excessive amounts of epoxy around the slots, but had the advantage over endmill and grinding bits in that square ended slots could be realized.

Fig. 18. Photograph of test cut of Z-slots in CFRP tube; note the texture of the plain weave CFRP prepreg.

VI. Conclusion

Z-slot resonant type narrow wall slotted waveguide antennas were investigated further using commercially available software, both as antennas and as load bearing hollow beam structures. Experimental work to further investigate both aspects is underway.

Acknowledgment

This UAV sensor work was inspired by the work of and numerous conversations with the late Professor R. Walker of QUT. Likewise, the work of the late Dr. B. da Costa of UC Irvine has been an inspiration.

The authors gratefully acknowledge the financial support of the National Natural Science Foundation of China (51203174) and Ningbo Natural Science Foundation (2013A610017). The authors are also indebted to EMSS SA for providing academic licenses of FEKO™ and a high level of technical support.

Also, the authors thank Mr. Hongsheng Zhang of NIMTE for manufacturing the CFRP tubes used in this work, and Dr. Yung-Tsang Chen of Nottingham University for his input on structural dynamics.

References

[1] D. Gray, J. Le Kernec and J. Thornton, "Assessment of Sochacki lenses for autonomous maritime patrol FLAR," accepted for *Int. RADAR Conf. 2014*, Lille, October 2014.

[2] M. Budde, M. Berning, M. Busse, T. Miyaki and M. Beigl, "The TECO Envboard: A mobile sensor platform for accurate urban sensing — And more," *Ninth Int. Conf. on Networked Sensing Systems (INSS)*, Antwerp, 2012.

[3] C.-D. Wu, P. MacNaughton, S. Melly, K. Lane, G. Adamkiewicz, J.L. Durant, D. Brugge and J.D. Spengler, "Mapping the vertical distribution of population and particulate air pollution in a near-highway urban neighborhood: Implications for exposure assessment," *J. of Exposure Sci. and Environmental Epidemiology*, no. 24, May/June 2014, pp. 297-304.

[4] D. Gray, K. Sakakibara and Y. Zhu, "Narrow-wall confined slotted waveguide structural antennas for small multi-rotor UAV," *Proceedings of the International Symposium on Antennas and Propagation - ISAP 2013*, Nanjing, October 2013, paper 332.

[5] X. Xin, Y. Zhu, D. Gray, Y. Qin and X. Fan, "Mechanical analysis of a structural novel slotted waveguide antenna for multi-rotor UAV," submitted to *The 1st International Conf. on Computational and Experimental Methods for Composite Materials and Structures*, Harbin University of Science and Technology, September 2014.

[6] W.H. Watson, "Resonant slots," *J. of the IEE, pt. IIIA: Radiolocation*, vol. 93, iss. 4, 1946, pp. 747 – 777.

[7] M.J. Ehrlich, "Slot-antenna arrays," Chapter 9 in *Antenna Engineering Handbook*, H. Jasik, Ed., McGraw-Hill, 1961.

[8] J.W. Sabat, "Structural response of the slotted waveguide antenna stiffened structure components under compression," *M.Sc. thesis of Air Force Institute of Technology*, Wright-Patterson Air Force Base, Ohio, March, 2010.

[9] J.T. Nemit, "Wideband dual-slot waveguide array," *United States Patent 3,740,751*, granted June 19th, 1973.

[10] W.J. Noble and J.W. Small, "Lightweight composite slotted-waveguide antenna and method of manufacture," *United States Patent 4,255,752*, granted March 10th, 1981.

[11] R.J. Chignell and J. Roberts, "Compact resonant slot for waveguide arrays," *Proc. Inst. Elec. Eng.,* vol. 125, no. 11, Nov. 1978, pp. 1213 - 1216.

[12] H.Y. Yee and P. Stellitano, "I-Slot Characteristics," *IEEE Trans. Antennas Propagat.,* vol. 40, no. 2, Feb. 1992, pp. 224 - 228.

[13] T. Sphicopoulus, "C-slot: A practical solution for phased arrays of radiating slots located on the narrow side of rectangular waveguides," *Inst. Elec. Eng. Proc.,*, pt. H, vol. 129, no. 2, Apr. 1982, pp. 49-55.

[14] D. Gray, K. Nicholson, K. Ghorbani and P. Callus, "Carbon Fibre Reinforced Plastic Slotted Waveguide Antenna", *Asia Pacific Microw. Conf. (APMC 2010)*, Yokohama, December 2010, paper WE4D-5.

[15] P.J. Callus and K.J. Nicholson, "Standard Operating Procedure - Manufacture of Carbon Fibre Reinforced Plastic Waveguides and Slotted Waveguide Antennas, Version 1.0," *Defense Science and Technology Organisation*, Australia, document: DSTO-TN-0937, June 2011.